MOTIONS OF CEPHEIDS
PERPENDICULAR TO THE GALACTIC PLANE

Akira M. Sinzi

Received March 20, 1961

Abstract

79 cepheids whose proper motions are provided by Morgan and Weaver, yield their means $\bar{z}=-31$ pc and $\overline{\dot{z}}=-6.3$ km sec $^{-1}$. Their distribution on $(z, \dot{z})$-plane suggests that cepheids of longer periods are older.

Dispersion of $\dot{z}$ component is estimated from the dispersion of radial velocities of 113 cepheids to be $\sigma_{\dot{z}}=5.6\pm 0.8$ km sec $^{-1}$. Simplfying Oort's method, these data yeild the z component of gravitational attraction of the galaxy at $z=100$ pc:

$$F(z)=(-1.8\pm 0.4)\times 10^{-9} \text{ cm sec}^{-2},$$

and the density of the matter in the vicinity of the sun:

$$\rho=(0.73\pm 0.15)\times 10^{-23} \text{ gr cm}^{-3}.$$

1. Distribution and Motion of Cepheids perpendicular to the Galactic Plane.

Since the cepheids are situated close to the galactic plane and move in accordance with the galactic rotation, it is difficult to remove the systematic terms within the galactic plane. We shall investigate the distribution and motions perpendicular to the galactic plane so as to obtain any information on general or individual properties of peculiar motions.

Materials of 79 cepheids adopted are those used in Sinzi's paper(1961), i.e.

Distance: Walraven, Muller and Oosterhoff (1958), Gascoign and Eggen (1957) and Janak (1958), reduced to Walraven, Muller and Oosterhoff's system.

Radial Velocity: Joy(1939) and Stibbs(1955).

Proper motion: Morgan and Weaver(1956).

At first, the equatorial rectangular components of motions are computed, then they are transformed into the galactic system through the formulae:

TABLE 1. SPACE MOTION OF CEPHEIDS.

WM	Star	r	μ	t	$\dot{x}'$	$\dot{y}'$	$\dot{z}'$	$\dot{x}$	$\dot{y}$	$\dot{z}$	$\dot{z}_p$	z
		kpc	″ 10^{-3}	km/sec 10^{-3}	km/sec	km/sec	km/sec	km/sec	km/sec	km/sec	km/sec	kpc
1	T U Cas	0.73	7	24	− 11.9	− 24.2	− 17.2	+ 21.7	− 22.7	+ 6.0	+ 12.3	−0.145
2	S U Cas	0.36	5	9	− 4.4	+ 6.1	− 7.7	− 6.8	− 8.3	− 0.7	+ 5.6	+0.053
3	R W Cam	2.19	26	270	+239.9	+ 37.2	−130.6	+ 75.1	− 1.4	−275.8	−269.5	+0.145
4	R X Cam	0.78	15	51	+ 44.1	− 11.0	− 49.2	+ 18.5	− 23.9	− 59.8	− 53.5	+0.064
5	S Z Tau	0.47	6	13	+ 1.2	+ 2.9	− 5.4	− 2.6	− 4.0	− 3.9	+ 2.4	−0.151
6	A W Per	0.93	3	13	− 4.5	+ 18.7	+ 0.9	− 19.2	+ 0.2	+ 1.4	+ 7.7	−0.087
7	R X Aur	1.31	9	56	− 31.1	+ 21.3	− 46.7	− 26.4	− 53.9	+ 1.9	+ 9.2	−0.030
8	S T Tau	1.24	13	76	+ 69.1	+ 3.0	− 34.1	+ 9.0	+ 2.0	− 76.6	− 70.3	−0.170
9	S V Mon	2.39	13	147	−132.5	+ 42.2	− 53.2	− 64.6	−104.3	+ 83.8	+ 90.1	−0.140
10	R S Ori	1.56	16	118	+ 92.2	+ 64.3	− 53.6	− 42.3	+ 0.6	−115.2	−108.9	+0.014
11	T Mon	0.86	10	41	− 39.2	+ 30.5	− 12.2	− 36.9	− 26.4	+ 23.7	+ 30.0	−0.039
12	R T Aur	0.52	13	32	− 9.7	+ 19.3	− 16.7	− 20.7	− 17.6	− 2.4	+ 3.9	+0.081
13	W Gem	0.81	14	54	− 45.0	+ 1.7	− 29.8	− 9.5	− 47.0	+ 24.9	+ 31.2	+0.050
14	ζ Gem	0.25	9	11	+ 7.8	+ 9.9	− 1.0	− 8.4	+ 3.5	− 8.8	− 2.5	+0.052
15	R Y CMa	1.23	16	93	− 94.7	+ 13.9	+ 21.1	− 30.2	− 24.1	+ 90.2	+ 96.5	+0.015
16	V X Pup	0.72	18	61	+ 21.5	− 2.4	− 58.3	+ 6.1	− 41.8	− 45.7	− 39.4	−0.017
17	X Pup	2.51	20	238	−150.2	+ 59.0	+174.2	− 84.2	+ 89.2	+203.6	+209.9	−0.011
18	A P Pup	1.67	28	221	+104.2	+170.6	+ 91.8	−149.9	+143.2	− 73.7	− 67.4	−0.087
19	A H Vel	0.49	11	26	+ 7.1	+ 33.7	− 12.4	− 32.0	− 4.8	− 17.2	− 10.9	−0.054
20	R S Pup	1.24	25	147	+111.1	+ 96.8	− 0.9	− 76.0	+ 58.4	−111.9	−105.6	+0.009
21	V Car	0.79	7	26	+ 18.8	+ 7.9	− 21.4	− 4.5	− 9.6	− 27.7	− 21.4	−0.160
22	R Z Vel	1.51	11	79	+ 55.6	+ 29.6	− 48.6	− 20.0	− 14.8	− 75.7	− 69.4	−0.034
23	S W Vel	2.58	17	207								−0.110
24	S X Vel	1.80	14	119	+ 84.0	+ 11.1	− 87.4	+ 3.7	− 37.5	−115.9	−109.6	−0.048
25	V Vel	1.07	8	41	+ 44.5	+ 20.8	+ 23.7	− 12.8	+ 43.2	− 30.8	− 24.5	−0.066
26	*l* Car	0.27	13	17	− 5.3	+ 5.4	+ 2.4	− 6.2	+ 0.1	+ 4.9	+ 11.2	−0.030
27	U X Car	1.56	13	96	+ 75.0	+ 46.1	− 44.8	− 32.3	− 1.1	− 93.5	− 87.2	+0.021
28	Y Car	1.48	9	63	− 5.4	+ 56.6	+ 23.5	− 56.7	+ 22.9	+ 7.0	+ 13.3	+0.008
29	U Car	1.34	15	95	− 47.0	− 73.1	+ 22.4	+ 63.8	− 7.9	+ 62.6	+ 68.9	+0.015
30	E R Car	0.90	9	38	+ 36.7	+ 18.9	+ 1.9	− 12.2	+ 20.2	− 33.9	− 27.6	+0.033
31	S Mus	0.64	17	52	− 37.6	+ 28.2	− 27.0	− 34.3	− 38.9	+ 15.7	+ 22.0	−0.078
32	T Cru	0.62	3	9	− 4.9	− 0.3	+ 9.5	− 0.5	+ 6.1	+ 8.8	+ 15.1	+0.010
33	R Cru	0.87	9	37	+ 33.6	− 21.4	− 2.2	+ 27.0	+ 11.8	− 26.9	− 20.6	+0.025
34	R Mus	0.82	8	31	+ 23.7	− 19.6	− 11.9	+ 23.4	− 1.2	− 23.2	− 16.9	−0.086
35	S Cru	0.70	11	37	+ 35.3	− 0.5	− 13.8	+ 6.6	+ 4.1	− 37.1	− 30.8	+0.061
36	X X Cen	1.41	11	73	+ 2.4	+ 72.2	− 1.3	− 70.7	+ 5.9	− 13.7	− 7.4	+0.130
37	v381 Cen	1.13	15	80	− 37.7	+ 64.1	+ 40.5	− 69.7	+ 23.6	+ 42.0	+ 48.3	+0.110
38	V Cen	0.74	11	39	+ 19.0	+ 39.3	+ 1.1	− 35.4	+ 13.0	− 22.0	− 15.7	+0.049
39	R TrA	0.67	16	51	+ 21.5	+ 44.0	− 11.0	− 39.6	+ 3.8	− 30.6	− 24.3	−0.085
40	S TrA	0.80	2	8	− 2.3	+ 6.0	− 9.3	− 6.3	− 8.8	− 3.3	+ 3.0	−0.110

TABLE 1. SPACE MOTION OF CEPHEIDS (Continued).

WM	Star	r	μ	t	$\dot{x}'$	$\dot{y}'$	$\dot{z}'$	$\dot{x}$	$\dot{y}$	$\dot{z}$	$\dot{z}_p$	z
		kpc	″ 10^{-3}	km/sec 10^{-3}	km/sec	km/sec	km/sec	km/sec	km/sec	km/sec	km/sec	kpc
41	U TrA	1.27	9	54	+ 49.7	− 21.9	+ 12.2	− 30.3	+ 32.0	− 34.1	− 27.8	−0.170
42	S Nor	0.66	3	9	− 9.0	− 6.4	+ 2.2	− 4.7	− 2.8	+ 9.8	+ 16.1	−0.058
43	R V Sco	0.76	11	40	+ 30.4	+ 7.4	+ 11.3	− 2.0	+ 24.6	− 22.2	− 15.9	+0.077
44	B F Oph	0.80	9	34	+ 13.7	+ 11.6	+ 41.1	− 9.0	+ 43.6	+ 5.6	+ 11.9	+0.120
45	X Sgr	0.32	9	14	+ 1.5	+ 18.4	− 5.6	− 17.8	− 2.7	− 6.7	− 0.4	+0.001
46	R Y Sco	0.93	28	123	+ 85.6	− 39.4	+ 83.5	+ 53.7	+110.0	− 29.3	− 23.0	−0.055
47	Y Oph	0.41	8	16	+ 0.4	+ 7.7	− 14.7	− 7.5	− 12.2	− 8.4	− 2.1	+0.071
48	W Sgr	0.40	9	18	+ 17.4	+ 23.8	+ 11.3	− 20.4	+ 20.0	+ 13.4	− 7.1	−0.028
49	A P Sgr	0.88	6	25	− 18.0	+ 22.6	− 8.3	− 25.4	− 13.7	− 8.3	+ 14.6	−0.038
50	W Z Sgr	1.54	28	204	+194.8	+ 41.4	− 58.5	− 6.9	+ 41.7	+203.3	−197.0	−0.039
51	Y Sgr	0.47	15	33	+ 15.0	+ 13.5	− 26.4	− 10.7	− 15.3	− 27.6	− 21.3	−0.018
52	X X Sgr	1.36	8	52	+ 36.2	+ 11.9	− 37.7	− 5.4	− 14.6	− 51.0	− 44.7	−0.045
53	U Sgr	0.57	11	30	− 0.7	+ 6.4	− 29.3	− 6.4	− 25.7	− 14.2	− 7.9	−0.046
54	S S Sct	0.95	14	63	− 61.3	+ 1.3	+ 19.7	− 12.0	− 10.8	+ 62.4	+ 68.7	−0.034
55	v350 Sgr	0.92	36	158	+150.7	+ 32.7	− 44.2	− 6.0	+ 33.3	−156.9	−150.6	−0.130
56	Y Z Sgr	0.93	6	26	− 21.4	− 22.2	− 5.4	+ 18.2	− 16.5	+ 19.5	+ 25.8	−0.120
57	B B Sgr	0.71	22	74	+ 29.2	+ 22.6	− 65.7	− 17.2	− 42.6	− 59.8	− 53.5	−0.110
58	F F Aql	0.33	8	12	− 6.7	+ 8.8	− 16.2	− 9.9	− 16.7	− 3.1	+ 3.2	+0.034
59	S Z Aql	1.79	7	59	− 34.3	− 19.8	− 42.2	− 13.5	− 54.7	+ 13.0	+ 19.3	−0.084
60	T T Aql	0.91	13	56	− 6.0	+ 2.9	− 56.2	− 3.9	− 52.2	− 21.6	− 15.3	−0.056
61	U Aql	0.55	14	36	+ 29.9	+ 19.6	− 4.3	− 14.1	+ 11.6	− 31.0	− 24.7	−0.110
62	U Vul	0.56	10	27	− 7.6	− 1.2	− 28.9	− 0.1	− 30.0	− 6.8	− 0.5	−0.008
63	S V Cyg	0.87	10	41	− 31.6	+ 41.8	+ 18.6	− 46.6	+ 5.2	+ 29.8	+ 36.1	+0.029
64	S V Vul	1.48	11	77	− 69.1	− 28.9	+ 5.1	+ 16.5	− 29.8	+ 66.9	+ 73.2	+0.007
65	η Aql	0.24	10	11	+ 0.8	+ 17.2	− 8.2	− 16.8	− 5.4	− 7.2	− 0.9	−0.056
66	S Sge	0.58	5	14	− 10.2	+ 3.3	− 13.5	− 5.1	− 16.3	+ 2.1	+ 8.4	−0.067
67	X Vul	0.99	12	56	+ 12.4	+ 43.6	+ 36.3	− 40.7	+ 41.4	− 0.4	+ 5.9	−0.023
68	C D Cyg	2.56	18	218	−114.6	+ 76.8	+165.2	− 95.5	+ 99.3	+105.5	+171.8	+0.067
69	S Z Cyg	2.78	14	185	−177.8	− 37.5	+ 51.4	+ 6.0	− 39.8	+184.6	+190.9	+0.189
70	X Cyg	0.85	17	68	− 51.1	− 46.5	+ 12.0	+ 36.9	− 16.8	+ 57.2	+ 63.5	−0.064
71	T Vul	0.59	5	14	− 11.7	− 3.6	+ 6.7	+ 1.5	+ 0.2	+ 13.9	+ 20.2	−0.104
72	V X Cyg	3.42	7	113	− 99.7	− 3.3	+ 50.4	− 14.1	− 1.9	+110.9	+117.2	−0.209
73	D T Cyg	0.45	8	17	− 14.1	− 9.2	+ 5.2	+ 6.6	− 2.7	+ 16.1	+ 22.4	−0.084
74	V Z Cyg	1.46	41	283	−214.8	−178.7	+ 65.1		+ 56.4	+244.8	+251.1	−0.216
75	Y Lac	2.38	9	102	+ 21.1	+ 98.7	+ 0.5	− 93.5	+ 18.2	− 33.3	− 27.0	−0.167
76	δ Cep	0.26	10	12	− 5.8	+ 15.4	− 11.2	− 16.2	− 11.3	− 2.7	+ 3.6	+0.002
77	R R Lac	2.11	20	200	+130.6	− 67.2	−141.0	+ 88.9	− 69.7	−169.6	−163.3	−0.074
78	V Lac	1.53	16	116	−109.8	− 27.1	+ 40.6	+ 7.6	− 17.1	+118.7	+125.0	−0.067
79	X Lac	1.10	14	73	+ 23.4	− 51.9	− 55.6	+ 55.2	− 42.6	− 38.6	− 32.3	−0.048

$\dot{x}'$, $\dot{y}'$, $\dot{z}'$: Equatorial rectangular components of motion.

$\dot{x}$, $\dot{y}$, $\dot{z}$: Galactic rectangular components of motion.

$\dot{z}_p = \dot{z} - \overline{\dot{z}}$

$$\dot{x} = \dot{x}' \cos\psi + \dot{y}' \sin\psi,$$
$$\dot{y} = -\dot{x}' \sin\psi \cos\theta + \dot{y}' \cos\psi \cos\theta + \dot{z}' \sin\theta,$$
$$\dot{z} = \dot{x}' \sin\psi \sin\theta - \dot{y}' \cos\psi \sin\theta + \dot{z}' \cos\theta,$$

in which φ , ψ and θ are Euler's angles, i.e.

$$\psi = \alpha_0 = 18^h\ 40^m, \quad \varphi^{I} = 0°, \quad \varphi^{II} = 32°.3, \text{ and}$$
$$\theta = 90° - \delta_0 = 62°.$$

Galactic latitude b^{II} in new system is adopted for the evaluation of z. Table 1 contains basic data, in which x– and y–axes direct to $l^I = 0°$ and $l^I = 90°$ on the galactic plane, respectively. We obtain from these data following means:

$$\overline{z} = -31 \text{ pc} \quad \text{with } \sigma_z = \pm 59 \text{ pc},$$
$$\overline{\dot{z}} = -6.3 \text{ km sec}^{-1} \text{ with } \sigma_{\dot{z}} = \pm 82 \text{ km sec}^{-1}.$$

The value of $\overline{z}$ is slightly greater than the value of 26 ± 7 pc for the distance of the sun from the galactic plane derived from radio observation by Westerhout(1957). The value of $\overline{\dot{z}}$ (Fig. 1) agrees with the z component $+6.3$ km sec^{-1} of the Dyer's basic solar motion: $v_0 = 15.3$ km sec^{-1} to $A=$ 262.4° and $D = +20.3°$ (1956).

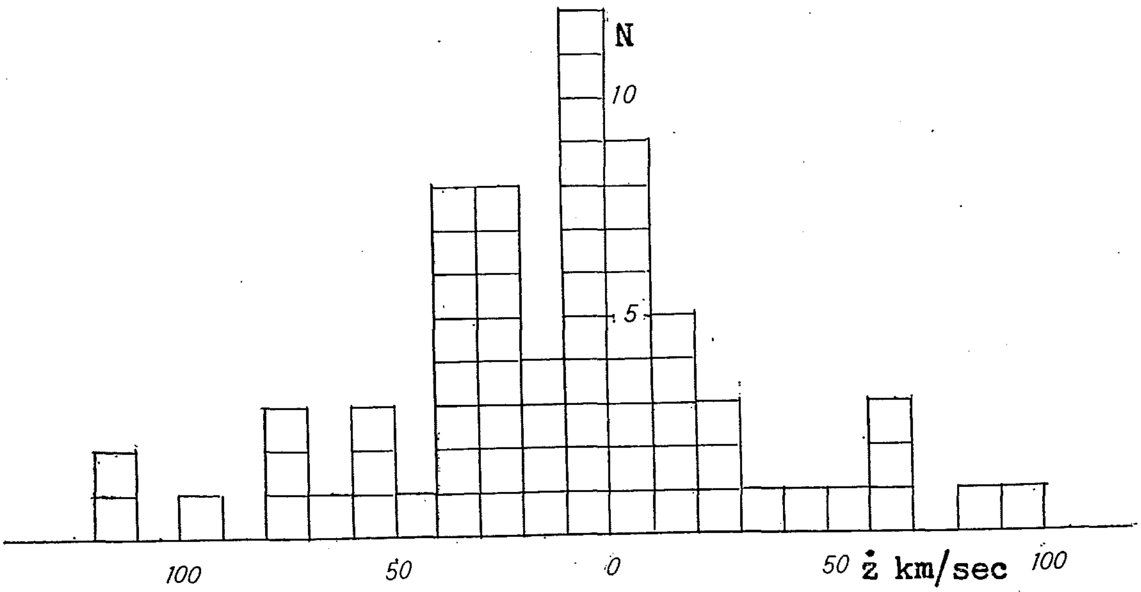

Fig. 1 Distribution of Cepheids Velocity

However, the dispersions obtained above are both large, perhaps, owing to the selection. In Fig. 2, the resultant values of proper motions are plotted for employed 78 stars. For smaller parallaxes, we find the stars of larger proper motions, which cause in Fig. 3, showing the relation between distance r and tangential velocity t, large values of t in long distances.

About one third of sample stars show exessively large values of tangential velocities for the ordinary classical cepheids. Hence, we cannot use these data straightly for any evaluation.

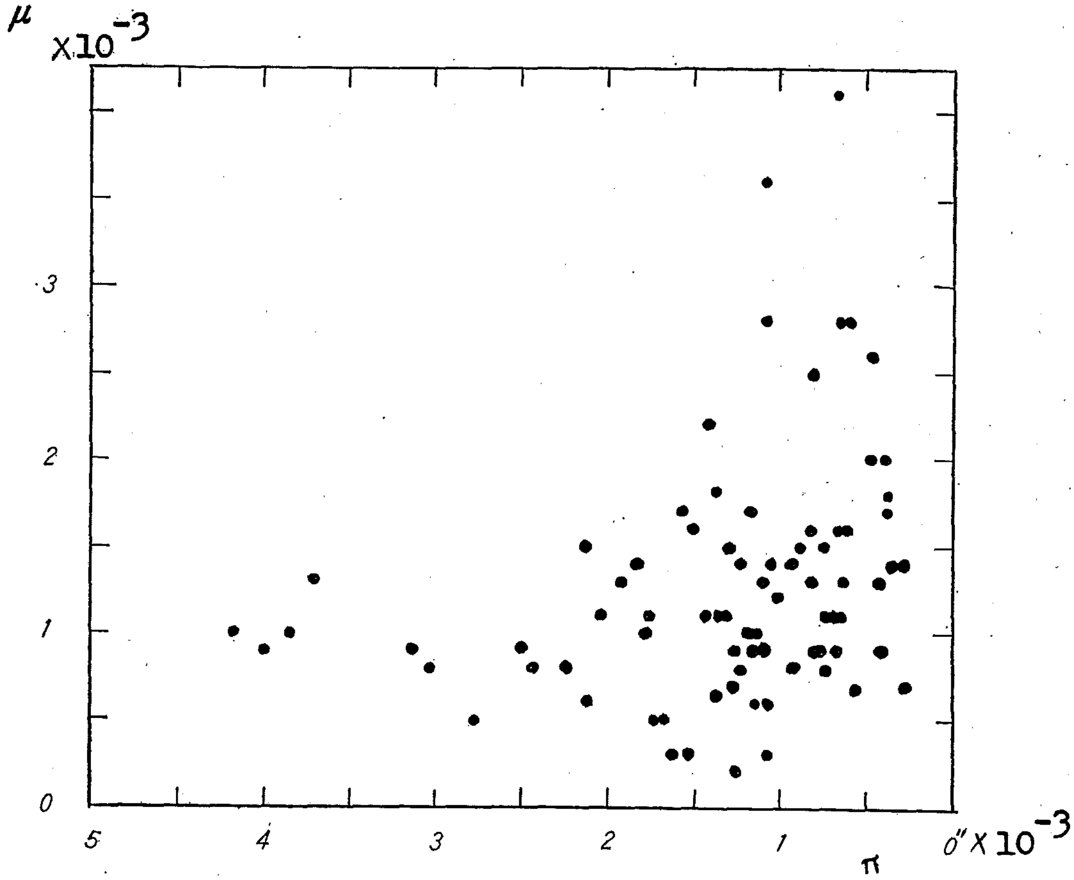

Fig. 2 Proper Motion of Cepheids

In Fig. 4, each cepheid is plotted by z and $\dot{z}$, with log P beside each. When we shift the coordinate axes to their means, which are shown by dotted lines, the stars locating in the first and third quadrants are receding from the galactic plane, while in the second and fourth quadrants are approaching to it. The numbers of these receding and approaching stars are shown in the histogram of Fig. 5, in which stars of high velocity component, i.e. $|\dot{z}| > 65$ km sec^{-1}, are omitted. In this figure, we can see that the cepheids of longer periods are, as a whole, approaching to the galactic plane, and opposite are the shorter periods. If we suppose that the cepheids are born very close to the galactic plane, and that, following Oort (1932), they are oscillating perpendicular to the galactic plane after their births, Fig. 5 seems to exhibit that the longer the period the older the cepheids.

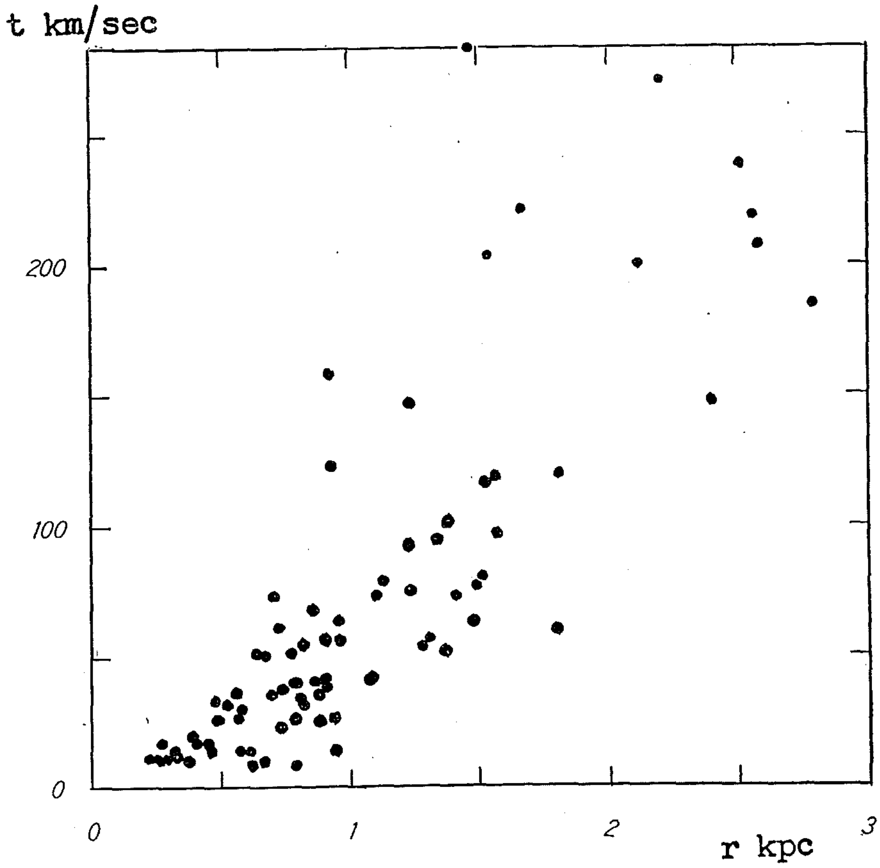

Fig. 3 Tangential Velocities of Cepheids

According to the current theory of stellar evolution, the brightest stars, which are situated on the zero age main sequence, at first, begin to turn-off and evolve to the right in *H–R* diagram, followded by stars in order of their brightness. If we assume, following Sandage(1958), that they enter the zone of pulsation on their horizontal traverse to the right, darker cepheids should be older than the brighters, since the brighter cepheids which has the same age as the darker should have had passed over the upper part of the pulsation zone far before. Darker cepheids are shorter in their periods. Then, the shorter period cepheids should be older. However, this is the situation seen at an epoch of time. If we look at one star, its period may become longer during its cepheid age, since the line of constant period in *H–R* diagram seems to be inclined downwards to the right (Arp, 1960). This inclination yields increase of period for about 30 per cent if cepheids evolve horizontally. In the absence of further data, we cannot attribute period distribution in Fig. 5 to this effect.

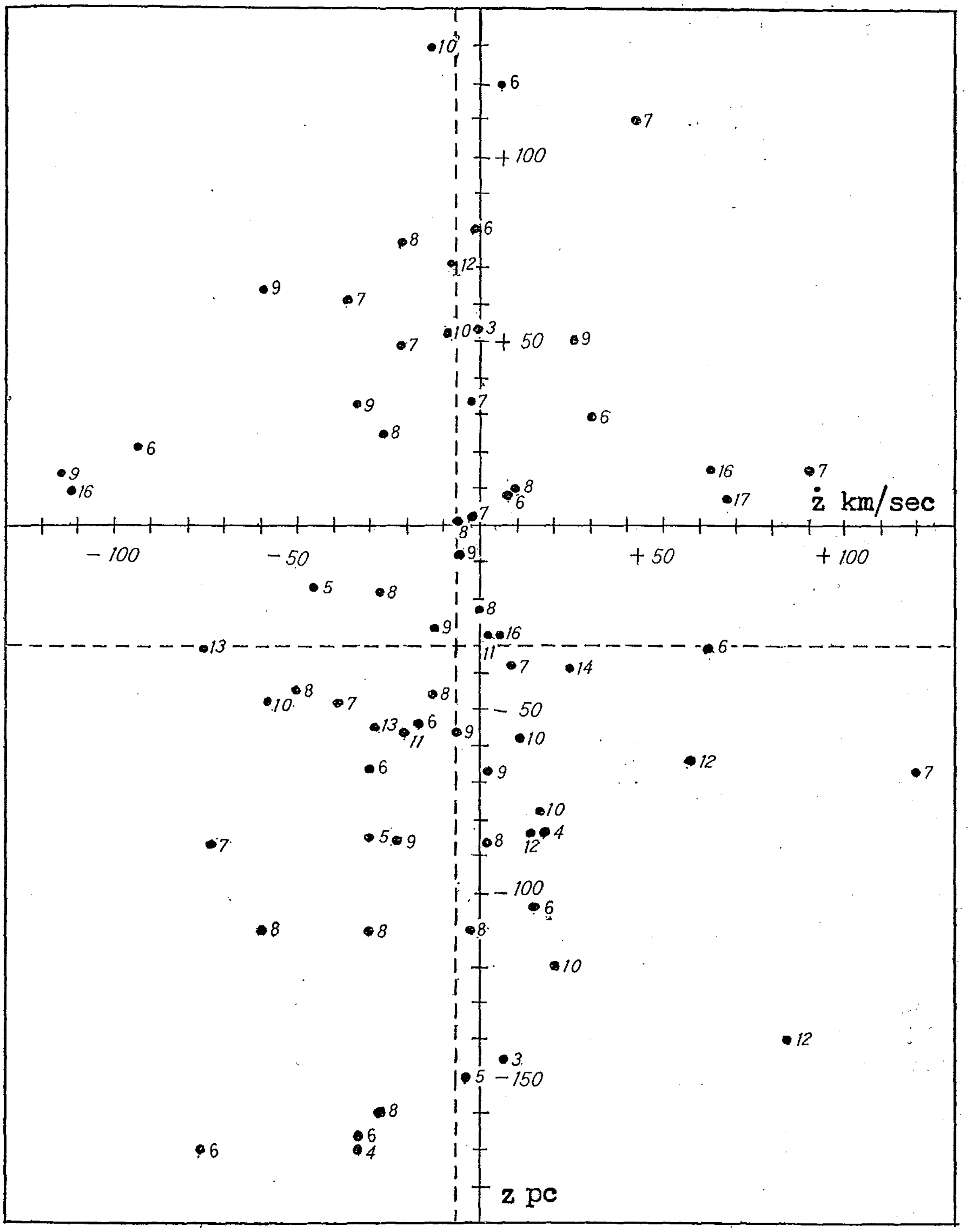

Fig. 4 Distribution of Cepheids on $(z—\dot{z})$-plane.
Attached numbers denote values of 10·log P.

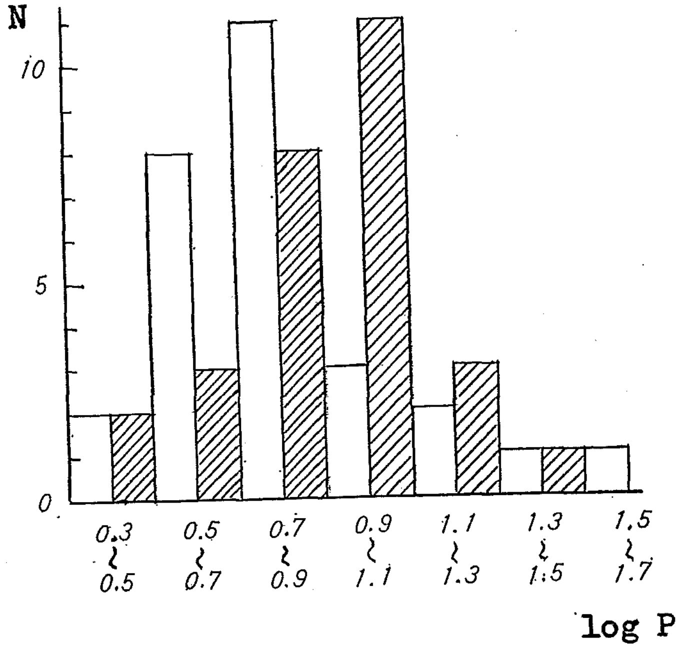

Fig. 5 Motions and Periods. Shaded and Open histograms are numbers of cepheids which are approaching to and receding from the galactic plane, respectively.

2. Analysis of Radial Velocity Data.

For simplicity we shall treat only stars which are situated on the galactic plane. Taking rectangular coordinate axes x, y on the plane, the radial velocity can be expressed, as shown in Fig. 6,

$$v = \dot{x} \cos\theta + \dot{y} \sin\theta, \qquad (1)$$

where θ is the position angle of the star.

Here, we shall suppose the frequencies of the components x, y of peculiar motion to be Gaussian:

$$\varphi(\dot{x}) = \varphi(\dot{y}) = \frac{h}{\sqrt{\pi}} e^{-h^2\dot{x}^2} = \frac{h}{\sqrt{\pi}} e^{-h^2\dot{y}^2} \qquad (2)$$

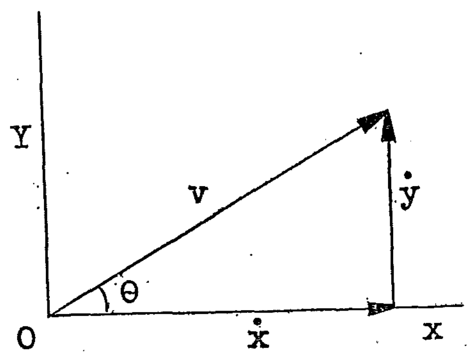

Fig. 6

with common dispersions. Then the frequency of combination of $(\dot{x}, \dot{y})$ is

$$F(\dot{x}, \dot{y}) = \varphi(\dot{x}) \cdot \varphi(\dot{y}) = \frac{h}{\sqrt{\pi}} e^{-h^2(\dot{x}^2+\dot{y}^2)} \qquad (3)$$

Hence, the frequency of radial velocity v in the direction θ can be expressed:

$$\psi(v) = \int_{-\infty}^{+\infty} F\{\dot{x}(v, \dot{y}), \dot{y}\} \left| \frac{\partial \dot{x}(v, \dot{y})}{\partial v} \right| d\dot{y}. \tag{4}$$

$\dot{x}$ is expressed in terms of v and $\dot{y}$ by (1)

$$\dot{x} = v \sec\theta - \dot{y} \tan\theta, \tag{5}$$

then (4) becomes

$$\psi(v) = \frac{2h^2}{\pi} e^{-h^2 \sec^2\theta \cdot v^2} \sec\theta \int_0^{\infty} e^{-h^2 (\dot{y}^2 \sec^2\theta - 2v\dot{y} \sin\theta \sec^2\theta)} d\dot{y}. \tag{6}$$

Put

$$\xi = h(\dot{y} \sec\theta - v \tan\theta) \tag{7}$$

and

$$\tau = hv \tan\theta, \tag{8}$$

then

$$h\dot{y} \sec\theta = \xi + \tau,$$

and

$$h^2 (\dot{y}^2 \sec^2\theta - 2v\dot{y} \sin\theta \sec^2\theta) = \xi^2 - \tau^2.$$

Therefore, (6) becomes

$$\psi(v) = \frac{2h}{\pi} e^{-h^2 v^2 \sec^2\theta} e^{\tau^2} \int_{-\tau}^{\infty} e^{-\xi^2} d\xi$$

$$= \frac{2h}{\pi} e^{-h^2 v^2} \int_{-\tau}^{\infty} e^{-\xi^2} d\xi$$

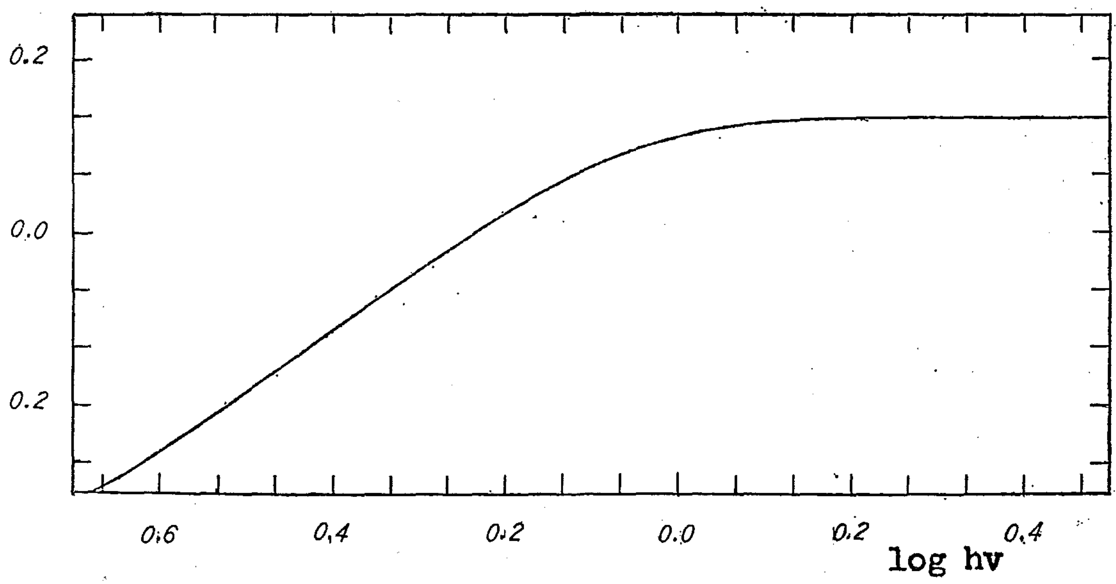

Fig. 7 Cumulative of $\Psi(v)/h$ in Logarithmic Scale.

$$= \frac{2h}{\pi} e^{-h^2 v^2} \left(\frac{\sqrt{\pi}}{2} - K(\tau)\right), \tag{9}$$

where

$$K(\tau) = \int_0^{\tau} e^{-x^2} dx.$$

Hence, the total frequency for radial velocity v is

$$\Psi(v) = \int_0^{2\pi} \psi(v, \theta)\, d\theta$$

$$= 4\int_0^{\pi/2} \psi(v, \theta)\, d\theta$$

$$= \frac{4h}{\sqrt{\pi}} e^{-h^2v^2} \left\{\frac{\pi^{3/2}}{4} - \int_0^{\pi/2} K d\theta\right\},$$

by (2), or using the error function Φ defined by

$$\Phi(x) = \frac{2}{\sqrt{\pi}}\int_0^{x} e^{-x^2} dx,$$

we have

$$\Psi(v) = \frac{4h}{\pi} e^{-h^2v^2} \frac{\sqrt{\pi}}{2}\left\{\frac{\pi}{2} - \int_0^{\pi/2} \Phi d\theta\right\}$$

$$= \frac{2h}{\sqrt{\pi}} e^{-h^2v^2} \left(\pi - 2\int_0^{\pi/2} \Phi\, d\theta\right). \tag{10}$$

Then, we have the relation between the frequencies of radial velocity v and of rectangular components $\dot{x}$, $\dot{y}$ of peculiar motion:

$$\Psi(v) = \frac{2h}{\sqrt{\pi}} e^{-h^2v^2} G, \tag{11}$$

TABLE 2. FUNCTION G.

hv	G	$\Psi(v)/h$
0.0	3.142	3.545
0.1	2.468	2.757
0.2	2.076	2.251
0.3	1.808	1.864
0.4	1.599	1.537
0.5	1.431	1.258
0.6	1.293	1.019
0.7	1.177	0.815
0.8	1.080	0.642
0.9	0.997	0.501
1.0	0.925	0.384
1.1	0.862	0.290
1.2	0.806	0.216
1.3	0.757	0.158
1.4	0.714	0.114
1.5	0.674	0.080
1.6	0.638	0.053
1.7	0.589	0.037
1.8	0.577	0.026
1.9	0.551	0.017
2.0	0.527	0.010
2.1	0.505	0.007
2.2	0.484	0.005
2.3	0.465	0.002
2.4	0.447	0.001
2.5	0.431	0.001
2.6	0.416	0.000
2.7	0.401	0.000
2.8	0.388	
2.9	0.375	
3.0	0.361	

where function G is defined by

$$G = \pi - 2\int_0^{\pi/2} \Phi\, d\theta. \tag{12}$$

The values of G and $\frac{\Psi(v)}{h}$ are given in Table 2, and in Fig. 7 the cumulative curve of $\frac{\Psi(v)}{h}$ is shown in logarithmic scales.

We can now estimate the distribution of peculiar motions perpendicular to the galactic plane. As the peculiar part of the radial velocites, we employ the recidual velocities appeared in Table 2 of Sinzi paper(1961), which are evaluated by subtracting the terms of the galactic rotation from the radial velocities.

In Fig. 8, are shown the frequency of these peculiar velocities, and are reproduced in Fig. 9 in logarithmic cumulative scales.

Adjusting the two curves of Figs. 7 and 9 so as to make them identical, we may take

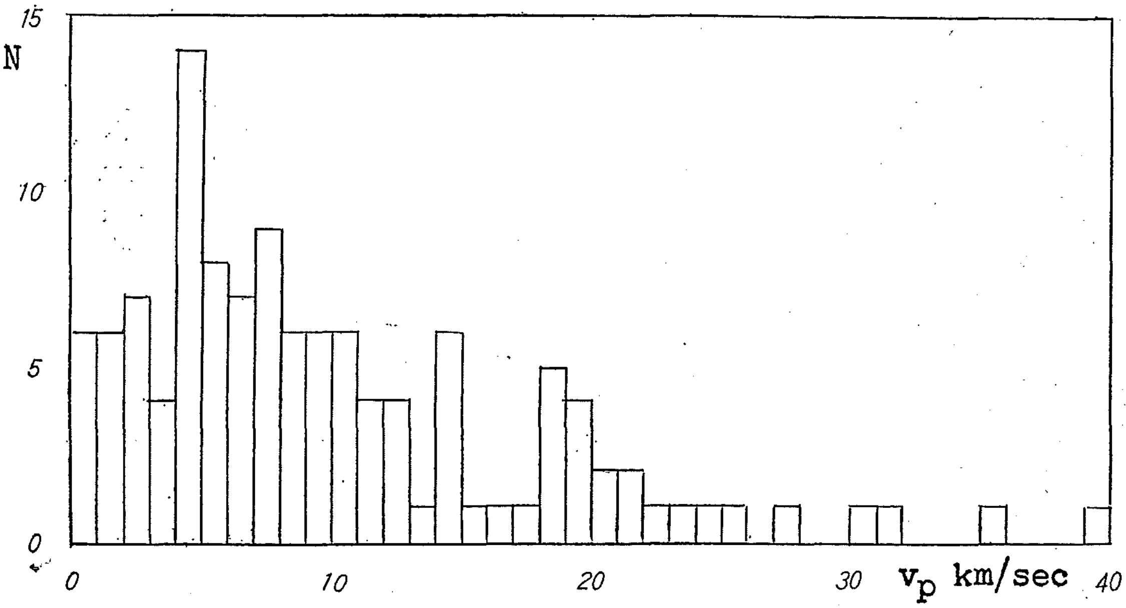

Fig. 8 Distributions of Peculiar Velocity

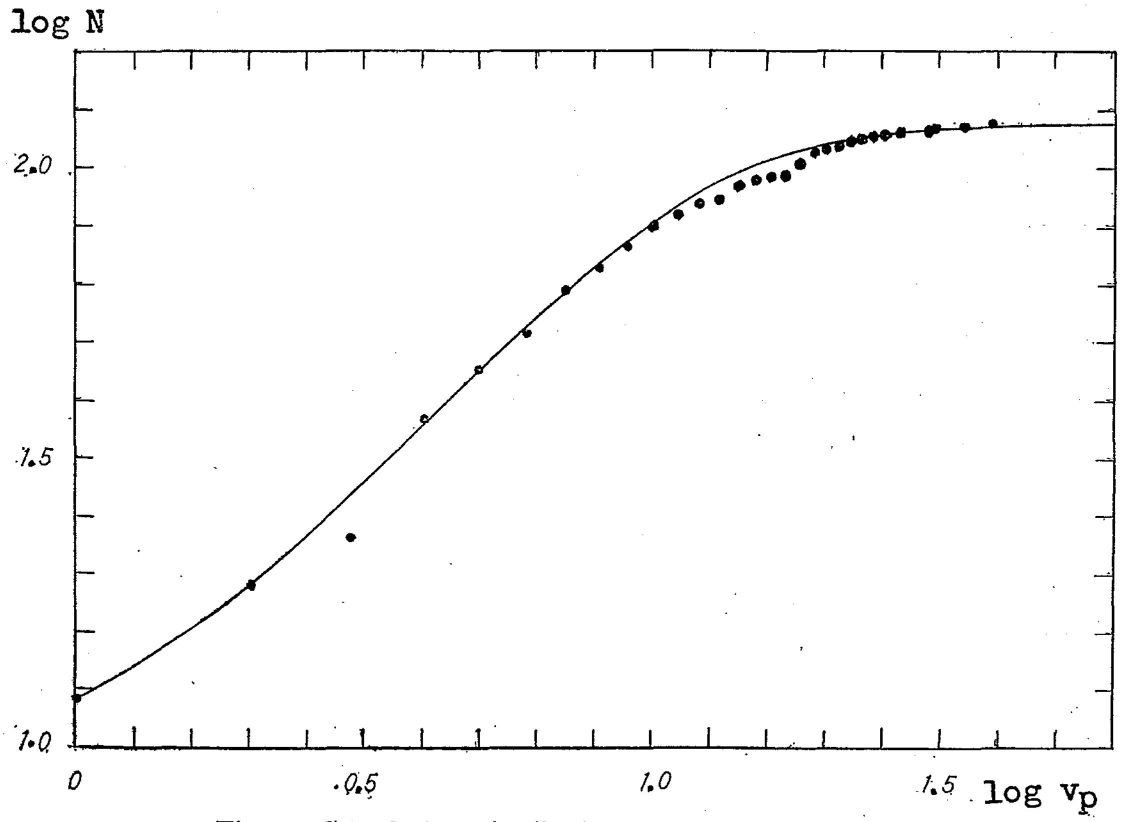

Fig. 9 Cumulative Distribution of Peculiar Velocity.

$$h = hv/v_p = 0.045 \pm 0.010,$$

in which error is estimated from the difference of two curves.

The dispersion of rectangular components of the peculiar velocities is, then

$$\sigma = 1/(h\sqrt{2}) = 11.2 \pm 1.6 \text{ km sec}^{-1}.$$

Considering that the length of z–axis of volocity ellipsoid is about a half of the lengths of x, y–axes, we may take

$$\sigma_{\dot{z}} = 5.6 \pm 0.8 \text{ km sec}^{-1}.$$

For the spatial distribution perpendicular to the galactic plane, we also employ the positions of the same 113 stars as above. Using b^{II} and the same weights as in the Sinzi's paper (1961) we obtain

$$\overline{z} = -\ 35.2 \text{ pc} \quad \text{with } \sigma_z = 76.4 \pm 5.6 \text{ pc}.$$

3. Potential of the Galaxy.

The energy integral of a star in the direction perpendicular to the galactic plane is:

$$H = \frac{1}{2}\dot{z}^2 + \kappa z^2.$$

Then, assuming the elliptic distribution of cepheids in $(z, \dot{z})$–plane, we have

$$\sqrt{2H} = \sigma_{\dot{z}} = 5.6 \pm 0.8 \text{ km sec}^{-1},$$

$$\sqrt{H/\kappa} = \sigma_z = 76.4 \pm 5.6 \text{ pc},$$

whence

$$H = 15.7 \pm 3.2 \text{ (km sec}^{-1})^2,$$

and

$$\kappa = (2.84 \pm 0.62) \times 10^{-30} \text{ (km sec}^{-1}\text{ sec})^2.$$

We denote by $F(z)$ the z component of the gravitational attraction of the galaxy, then

$$\kappa z^2 = -\int_0^z F(z)\, dz,$$

from which we have

$$F(z) = -\ 2\kappa z.$$

Using the value of κ obtained just above, we obtain

$$F(z) = (-\ 0.57 \pm 0.12) \times 10^{-29} z \quad \text{cm sec}^{-2}\text{ cm}^{-1},$$

or,

$$F(z) = (-\ 1.76 \pm 0.37) \times 10^{-11} z \quad \text{cm sec}^{-2}\text{ pc}^{-1},$$

Following Kusmin(1955), we define a galactic parameter C by

$$C^2 = -\left(\frac{\partial^2 \Phi}{\partial z^2}\right)_{z=o},$$

where Φ is the galactic potential. Then, we can obtain the density ρ of matter in the galactic plane by the formula

$$4\pi G\rho = C^2 - 2(A^2 - B^2).$$

We have

$$C^2 = 2\kappa$$
$$= (0.57 \pm 0.12) \times 10^{-29} \quad \text{cm}^2\ \text{sec}^{-2}\ \text{cm}^{-2},$$

and

$$C = 73.6 \pm 7.7 \quad \text{km sec}^{-1}\ \text{kpc}^{-1}.$$

Further, employing the values of A and B by Sinzi(1961),

$$A = \quad 14.3 \pm 0.8 \text{ km sec}^{-1}\ \text{kpc}^{-1},$$

$$B = -\ 19.7 \pm 5.9 \text{ km sec}^{-}\ \text{kpc}^{-1},$$

we obtain

$$\rho = (0.73 \pm 0.15) \times 10^{-23} \quad \text{gr cm}^{-3}.$$

4. Conclusions.

For 79 cepheids, the means of the positions and motions perpendicular to the galactic plane are:

$$\overline{z} = -31 \text{ pc} \quad \text{with } \sigma_z = \pm\ 59 \text{ pc},$$

$$\overline{\dot{z}} = -\ 6.3 \text{ km sec}^{-1} \quad \text{with } \sigma_{\dot{z}} = \pm\ 82 \text{ km sec}^{-1}.$$

The distribution of these stars on the $(z, \dot{z})$-plane shows that cepheids of longer periods are generally approaching to the galactic plane while cepheids of shorter periods are receding from it.

The dispersion of the motions perpendicular to the galactic plane is estimated from the dispersion of the radial velocities to be

$$\sigma_{\dot{z}} = 5.6 \pm 0.8 \text{ km sec}^{-1},$$

which yields the z-component of gravitational attraction of the galaxy

$$F(z) = (-\ 1.8 \pm 0.4) \times 10^{-9} \quad \text{cm sec}^{-2} \quad \text{at } z = 100 \text{ pc}.$$

And the density of matter in the vicinity of the sun

$$\rho = (0.73 \pm 0.15) \times 10^{-23} \quad \text{gr cm}^{-3}.$$

References.

Arp, H. 1960, *A. J.* **65**, 404.

Dyer, E. R. 1956, *A. J.* **61**, 233.

Gascoign, S. C. B. and Eggen, O. J. 1957, *M. N.* **117**, 430.

Janak, F. 1958, *B. A. C.* **8**, 107.

Joy, A. H. 1939, *Ap. J.* **89**, 356.

Kusmin, G. 1956, *A. J. U. S. S. R.* **33**, 27.

Oort, J. H. 1932, *B. A. N.* **6**, 249.

Sandage, A. 1958, *Ap. J.* **127**, 513.

Sinzi, A. M. 1961, *Contr. Mar. Res. Lab., J. H. O.* **2**, 171.

Stibbs, D. W. N. 1955, *M. N.* **115**, 363.

Walraven, Th., Muller, A. B. and Oosterhoff, Th. 1958, *B. A. N.* **14**, 81.

Weaver, H. F. and Morgan, H. R. 1956, *A. J.* **61**, 268.

Westerhout, G. 1957, *B. A. N.* **13**, 201.